NUMERICAL SIMULATION OF GRAVITY CURRENTS

Akhilesh Kumar JHA[1], Juichiro AKIYAMA[2] and Masaru URA[3]

[1] Member of JSCE, Dr. Engr., Instructor, Dept. of Civil Engineering, Kyushu Institute of Technology
(Sensui Cho 1-1, Tobata, Kitakyushu 804-8550, Japan)
[2] Member of JSCE, Ph.D., Professor, Dept. of Civil Engineering, Kyushu Institute of Technology
[3] Member of JSCE, Dr. Engr., Professor, Dept. of Civil Engineering, Kyushu Institute of Technology

The motion of 2D gravity currents on a horizontal bed is simulated by a Large Eddy Simulation (LES) model. The gravity currents consist of either a mixture of nearly uniform sized particles or saline water. The numerical model uses cubic spline method for space derivatives and Crank-Nicolson scheme with fractional step for marching in time. The eddy viscosity is computed by Smagorinsky method modified to include effects of buoyancy. The simulated results are compared with experimental data for front height, front propagation speed and front buoyancy. The computed densimetric Froude number at the front is compared with experimental value as well as that available from existing empirical and experimental studies. The numerical model shows promising results for simulation of gravity currents and understanding front characteristics.

Key Words : *Gravity current, numerical simulation, LES, cubic spline, Smagorisnky SGS.*

1. INTRODUCTION

One fluid flowing into another fluid of different density under the influence of gravity is termed as gravity current. Turbidity currents and discharge of industrial waste into rivers and sea are typical examples of gravity currents. In a laboratory, such gravity currents may be generated by suddenly removing the barrier separating two fluids of different density. The lighter fluid may be the fresh water while the denser fluid may be saline water of varying concentration or a water particle mixture. The importance of studying various aspects of the motion of a gravity current needs no overemphasis[1].

A large number of experimental studies aimed at formulating some simplified models for gravity currents have been reported so far[1,2,3]. Huppert and Simpson[2] described the denser fluid released into less dense ambient fluid as collapse of a series of equal area rectangles and proposed a constant Froude number for the moving front, $F_{is} = 1.19$ as long as the ratio of the height of front to the depth of ambient fluid, $H/h \leq 0.075$ and $F_{is} = 0.5(H/h)^{-1/3}$ otherwise. Rottman and Simpson[3] latter revised some of the conclusions of Huppert and Simpson[2], particularly the description of the slumping of denser fluid as the collapse of a series of equal area rectangles and transition from initial adjustment phase, with approximately constant front speed, to an eventual self-similar phase, with a gradually decreasing front speed. Bonnecaze et al.[4] numerically studied particle-driven gravity currents by a single as well as double-layer model based on shallow water equations. However, modeling based on shallow water equations have obvious limitations in simulating turbulence phenomena. Klemp et al.[5] studied factors regulating propagation and structure of gravity currents comparing various approaches to research on gravity currents.

The motion of 2D gravity currents on a horizontal bed is particularly difficult for numerical treatment as the gravity current has to form from a static state. Nakayama and Satoh[6] simulated plumes advancing over horizontal surfaces by Large Eddy Simulations (LED) and categorized the motion in three phases called immature state, transition state and subtle state. Hosda et al.[7] numerically studied induced internal waves in a densimetric exchange flow. Akahori et al.[8] proposed a two-dimensional model using CIP[9,10] for gravity currents. They studied the front shape for a rather small range of the ratio of the depth of gravity current to the depth of ambient fluid. Moreover, front velocity and front buoyancy was not discussed there. In the above three studies very limited verification of numerical results was performed against experimental data.

This study examines experimentally and numerically the motion of 2D suspension and saline gravity currents on a horizontal bed. The gravity currents are generated by releasing denser fluid into a less dense ambient fluid by opening a gate. Particularly the densimetric Froude number of the front as a function of velocity, buoyancy and height is compared with that given by Huppert and Simpson[2]. The focus is to understand how velocity, buoyancy, height of the front and densimetric Froude number vary in relation to each other as the front moves forward. A Large Eddy Simulation (LES) model is developed with cubic spline for space and Crank-Nicolson scheme with fractional step for time. The numerical results are compared with substantial experimental data and important conclusions are drawn about applicability of the numerical model and motion of the front.

2. MODEL DESCRIPTION

Applying the grid-filter to the incompressible Navier-Stokes equations and mass transport equation, the governing equations for the mean-flow and mass transport are obtained as

$$\frac{\partial U_i}{\partial x_i} = 0 \tag{1}$$

$$\frac{\partial U_i}{\partial t} + U_j \frac{\partial U_i}{\partial x_j} = -\frac{1}{\rho_a}\frac{\partial P}{\partial x_i} + \nu \frac{\partial^2 U_i}{\partial x_j^2} + \frac{\partial}{\partial x_j}\left(-\overline{u_i' u_j'}\right) + g_i \frac{\Delta\rho}{\rho_a} \tag{2}$$

$$\frac{\partial C}{\partial t} + (U_i + V_{si})\frac{\partial C}{\partial x_i} = \frac{\partial}{\partial x_i}\left(-\overline{u_i' c'}\right) \tag{3}$$

where U_i= velocity component in the x_i direction, P = pressure in excess of the hydrostatic pressure at reference density ρ_a, $\Delta\rho$ = density excess ($=\rho-\rho_a$), ρ = total density, g_i= specific body force in the x_i direction, u_i' = fluctuating velocity, C = volume concentration of particles or dense fluid, c'= fluctuating concentration; $\overline{u_i' u_j'}$ = subgrid correlation terms between fluctuating velocity due to the grid-filtering, $\overline{u_i' c'}$ = subgrid correlation terms between fluctuating velocity and concentration and V_{si} = settling velocity of particles in the x_i direction. $-\overline{u_i' u_j'}$ can be expressed as

$$-\overline{u_i' u_j'} = \nu_t\left(\frac{\partial U_i}{\partial x_j} + \frac{\partial U_j}{\partial x_i}\right) - \frac{2}{3}k\delta_{ij} \tag{4}$$

where ν_t = subgrid scale eddy viscosity; k = turbulent kinetic energy ; δ_{ij}= Kronecker delta function. The last term in Eq.(4) represents the normal stresses and can be absorbed in the pressure terms of the momentum equations.

Assuming that the sub-grid turbulent production includes a buoyancy term[11], subgrid scale eddy viscosity ν_t can be expressed as

$$\nu_t = (Cs\Delta)^2\left(|\bar{S}|^2 - \frac{g_i}{\rho Sc_t}\frac{\partial \Delta\rho}{\partial x_i}\right)^{1/2} \tag{5}$$

where Δ= filter width, Cs = Smagorinsky constant and Sc_t = subgrid turbulent Schmidt number. The magnitude of large-scale strain is given by

$$|\bar{S}| = \left(2\bar{S}_{ij}\bar{S}_{ij}\right)^{1/2} \tag{6}$$

$$\bar{S}_{ij} = \frac{1}{2}\left(\frac{\partial U_i}{\partial x_j} + \frac{\partial U_j}{\partial x_i}\right) \tag{7}$$

The correlation term in Eq.(3) is generally assumed to be expressed as

$$-\overline{u_i' c'} = \frac{\nu_t}{Sc_t}\frac{\partial C}{\partial x_i} \tag{8}$$

Applying operator splitting technique, Eq.(2) can be written as a advection-diffusion equation

$$\frac{\partial \bar{U}_i}{\partial t} + U_j\frac{\partial \bar{U}_i}{\partial x_j} = 2\frac{\partial}{\partial x_j}\left[(\nu + \nu_t)\bar{S}_{i,j}\right] \tag{9}$$

and a pressure equation

$$\frac{\partial U_i}{\partial x_i} = 0 \tag{10}$$

$$\frac{\partial \bar{U}_i}{\partial t} = -\frac{1}{\rho_a}\frac{\partial P}{\partial x_i} + g_i\frac{\Delta\bar{\rho}}{\rho_a} \tag{11}$$

The pressure is computed by the Poisson equation, derived from Eqs.(10) and (11).

In the simulation of particle clouds, the model treats the particle phase as a continuous fluid and the drift velocity between fluid phase and particle phase is assumed to be the settling velocity of particles. This model, efficient when particles are relatively finer and the cloud is relatively denser, has been used successfully by Li[12] for numerical studies of convection of particle thermals and by Celik and Rodi[13] for sediment transport in open channels.

3. COMPUTATIONAL TECHNIQUE

The governing equations are numerically integrated by evaluating space derivatives by a

cubic spline and advancing the solution in time by the Crank-Nicolson scheme. A similar model was applied by Ying et al.[14] to heavy turbulent thermals. However, in order to reduce the computation time in iterative Crank-Nicholson scheme, we use the Crank-Nicolson scheme with fractional step. The steps in time-integration scheme are

$$\text{Step 1: } f^{t+\Delta t/2} = f^t + 0.5\Delta t.f(v^t) \quad (12)$$

$$\text{Step 2: } f^{t+\Delta t} = f^t + 0.5\Delta t.f(v^{t+\Delta t/2}) \quad (13)$$

4. EXPERIMENTS

Experiments were conducted in a flume made of plexiglass, 7.5m long, 0.1m wide and 0.9 m deep (Fig.1). The ambient fluid is fresh water with density ρ_a. The density currents were generated by opening the gate that separated the ambient fluid from either a water-particle mixture or saline water with density ρ_0, initial total buoyancy W_0 and initial square shaped area A_0 (=a x a). Results for four sets of experiments are presented here – two with saline water and two with water particle mixture. The depth of ambient fluid, h in all cases is 0.9m. The initial buoyancy W_0 and the relative density difference, $\varepsilon_0 = (\rho-\rho_a)/\rho_a$ for the four cases are as follows;

Table 1: Experimental Conditions

Case	W_0 (cm^3/s^2)	A_0 (cm^2)	a (cm)	ε_0
GP2-1	4900	1296	36	0.040
GP2-2	6860	1296	36	0.140
GS2-1	7940	900	30	0.009
GS2-2	9700	900	30	0.011

GP denotes experiments with water-particle mixture and GS denotes experiments with saline water.

The motion of the front of the gravity currents was tracked by a CCD camera and front velocity, area of the front and height of the front were obtained from the recorded images. Each experiment was repeated five times under the same experimental conditions and the data presented herein are the average of such five runs. The buoyancy of the front at a given location was obtained by cutting off the front from the rest of the front by inserting a sheet behind the front and siphoning out the deposited particles after they fully settle down on the bed. In case of saline water, buoyancy of the front was estimated from the density distribution measured by conductivity meters. For a given location, three such measurements were taken for the front buoyancy and the data given here are average of such three measurements.

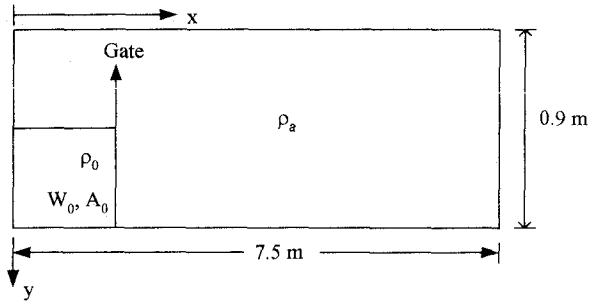

Fig.1 Experimental setup.

5. NUMERICAL RESULTS

The numerical model was applied to simulate the motion of the gravity currents observed experimentally as explained above. The physical domain was divided into computational cells of 0.01m x 0.01m. The Smagorinsky constant, C_s=0.16, known for 3D computations, is also used here. The turbulent Schmidt number, S_{ct} = 0.1 was used, which is low compared to the usual range of 0.4-1.0. However, S_{ct} =0.1 gave better results, the reason for which would be investigated in future. The time step was so chosen as to provide a stable computation. The positive x-direction points to the right and the positive y-direction to the down (Fig.1). All boundaries were set no-slip giving both normal and tangential velocities at the boundaries as zero.

Fig.2 presents a sequence in the motion of the front as computed by the numerical model for the case GP2-1. It is observed that the shape of the front as it moves forward is reasonably produced by the numerical model. The billow formation behind the front can also be seen in the figure.

The computed results for front velocity, front height and front buoyancy for saline gravity currents, cases GS2-1 and GS2-2, are compared with experimental data in Figs.3-5 and that for suspension gravity currents, cases GP2-1 and GP2-2, in Figs.6-8. In the figures, the lines and symbol show computed and experimental results, respectively. The plots show non-dimensional front

velocity, front height and front buoyancy against the non-dimensional front location. We have defined a front location X_i beyond which the front is well developed, uninfluenced by the largely inactive part of the current behind the front and it moves on its own. The following non-dimensional parameters are thus defined;

$$X^* = X_f / h \quad ; \qquad U^* = \frac{U_f}{\left(W_i^2 / A_i\right)^{1/4}}$$

$$H^* = \frac{H}{A_i^{1/2}} \quad ; \qquad B^* = \frac{B}{\left(W_i / A_i\right)}$$

where X_f = front location relative to the point X_i, W_i and A_i = Total buoyancy and area, respectively, of the front at X_i, U_f = front velocity, H = front height and B = front buoyancy. Before X_i, the height of the front falls rapidly and so does the front velocity. This phase is not shown in the figure as we want to focus on relatively stable and well developed phase of the motion of gravity current.

The agreement between experimental data and computed results are overall reasonable. It is seen from Fig.3 that the front velocity of saline gravity currents shows a gradual but continuous slowdown. However, front velocity of suspension gravity currents drops very slowly or remains more or less constant for some distance followed by a rather steep slowdown beyond a point (Fig.6). The height of saline gravity current remains almost constant as it moves forward whereas that of suspension gravity current shows continuous reduction (Figs.4,7). The computed buoyancy of both saline and suspension gravity current front changes very slowly. Although experimental data shows a rather steep drop in front buoyancy towards the end, computed results differ on this account. It is felt that beyond a certain point, the front velocity and buoyancy decrease rather rapidly. The significance, reason or the physical meaning of this point of a sudden change in the front characteristics are not well known at this time. However, it may be speculated that the front looses its buoyancy significantly at some point in space and time, which manifests as sudden drop in front velocity and height.

It may be remarked that the computed results exhibit some numerical oscillations towards advanced time which can be rectified by using finer discritization in space and time.

Figs.9 and 10 compares experimental and

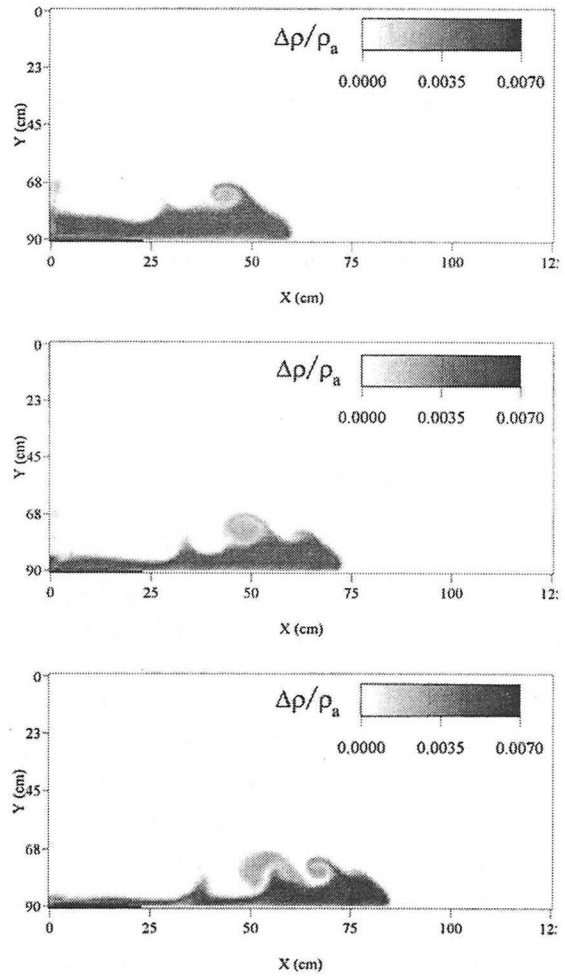

Fig.2 Computed motion of front for the case GP2-1.

computed front densimetric Froud numbe F_i given by Eq.17 with F_{is} given by Huppert and Simpson[2] (see Section 1:Introduction).

$$F_i = \frac{U_f}{\sqrt{BH}} \qquad (17)$$

It may be seen that both experimental data and the computed results cluster around the line given by Huppert and Simpson[2] but don't exactly follow that. It is also seen that the data for suspension gravity current show a larger scatter than the data for saline gravity current. It is understood that the densimetric Froude number remains more or less constant for a given front height, specially in case of saline gravity current, under a given depth of ambient fluid, even though the front velocity and buoyancy changes as the front advances. More detailed investigation is required to gain further insight into this.

6. CONCLUSIONS

The motion of gravity currents on a horizontal bed, produced by releasing denser fluid into a less

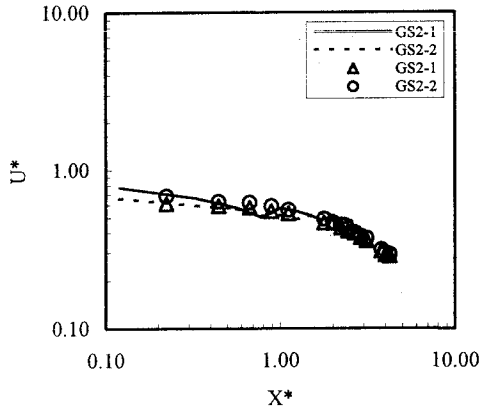

Fig.3 Front velocity saline gravity current.

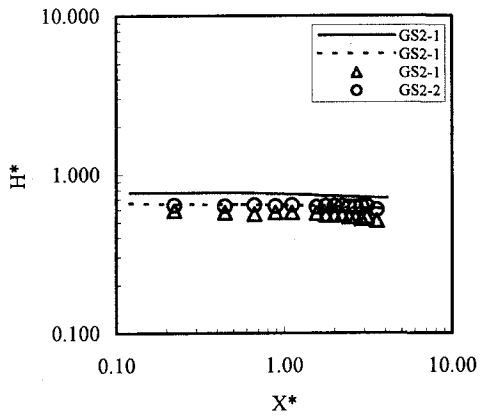

Fig.4 Front height for saline gravity current.

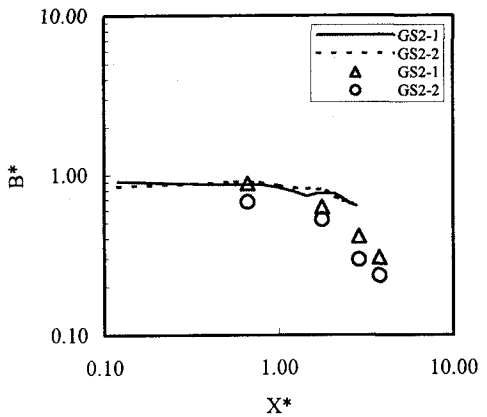

Fig.5 Front buoyancy for saline gravity current.

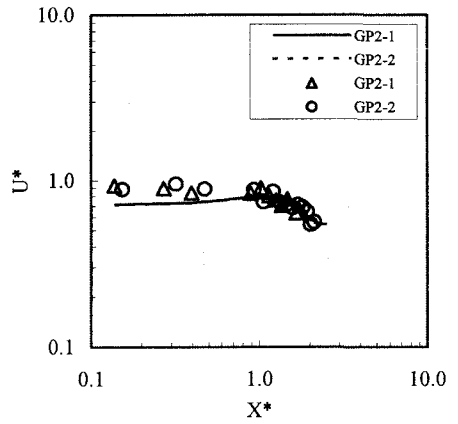

Fig.6 Front velocity for suspension gravity current.

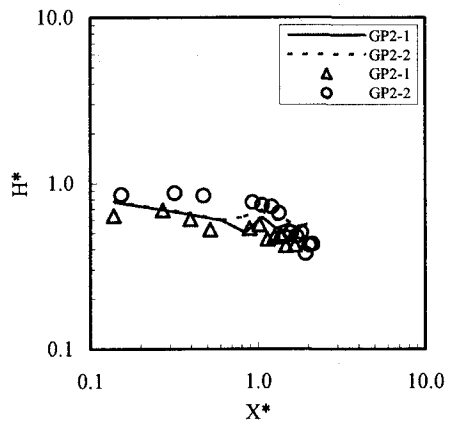

Fig.7 Front height for suspension gravity current.

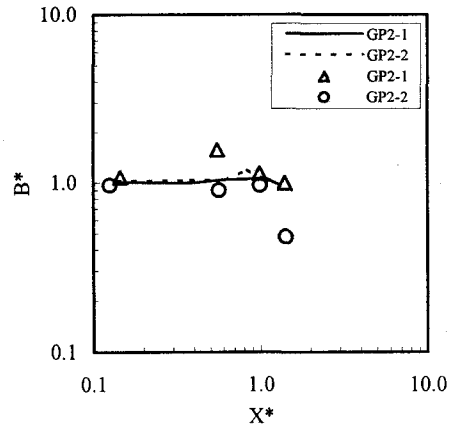

Fig.8 Front buoyancy for suspension gravity current.

dense fluid by opening a gate, is simulated by a Large Eddy Simulation (LES) model. Suspension and saline gravity currents are considered. The numerical model uses cubic spline for space and Crank-Nicolson scheme with fractional step for time. The Smagorinsky method, modified to include effects of buoyancy, is used to compute the eddy viscosity. The simulated results are compared with experimental data for front height, front propagation speed and front buoyancy. The computed densimetric Froude number is compared with experimental value as well as that available from existing studies.

It is concluded that the numerical model

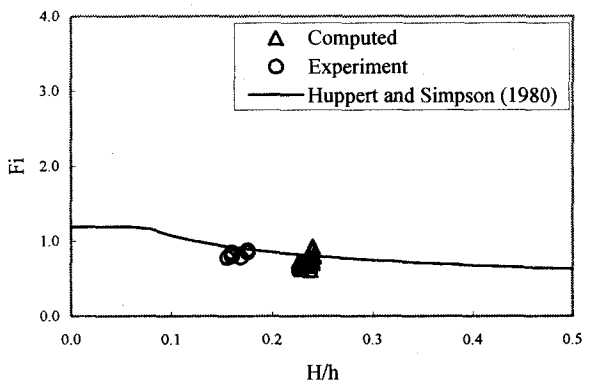

Fig.9 Densimetric Froude number of front for saline gravity current..

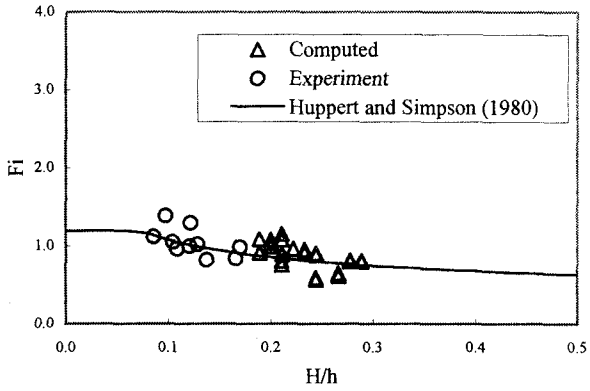

Fig.10 Densimetric Froude number of front for suspension gravity current.

presented herein can reasonably simulate the motion of a 2D gravity current. On the motion of gravity current it is observed that the front velocity and buoyancy shows a steep decrease after a particular point in space. However, the densimetric Froude number remains more or less unchanged for a given front height. These would be studied in further detail in our future works.

ACKNOWLEDGMENT

This study was supported by the Grant-in-Aid for Science Research of the Ministry of Education and Culture, Japan under the Grant B(2) 12555149.

REFERENCES

1. Simpson, J. E.: *Gravity Currents: In the environment and the laboratory, Ellis Horwood,* 1987.
2. Huppert, H. E. and Simpson, J. E.: The slumping of gravity currents, *J. Fluid Mech.*, Vol.99, part 4, pp.785-799, 1980.
3. Rottman, J. W. and Simpson, J. E.: Gravity currents produced by instantaneous release of a heavy fluid in a rectangular channel, *J. Fluid Mech.*, Vol.135, pp.95-110, 1983.
4. Bonnecaze, R. T., Huppert, H. E. and Lister, J. R.: Particle-driven gravity currents, *J. Fluid Mech.*, Vol.250, pp.339-369, 1993.
5. Klemp, J. B., Rotunno, R. and Skamarock, W. C.: On the dynamics of gravity currents in a channel, *J. Fluid Mech.*, Vol.269, pp.169-198, 1994.
6. Nakayama, K. and Satoh, T.: Analysis of plumes on horizontal surface by LES model, *Journal of Hydraulic, Coastal and Environmental Engineering*, JSCE, No.628/II-48, pp.97-114, 1999.
7. Hosada, T., Nishizawa, K., Fukusumi, A., Okubo, K. and Muramoto, Y.: Numerical studies on internal waves induced in a densimetric exchange flow, *Annual Journal of Hydraulic Engineering*, JSCE, Vol.40, pp.525-530, 1996.
8. Akahori, R., Shimizu, Y. and Nakayama, S.: Numerical calculation of flow and mixing in vertical boundary surface of density, *Annual Journal of Hydraulic Engineering*, JSCE, Vol.43, pp.521-526, 1999.
9. Takewaki, H., Nishiguchi, A. and Yabe, T.: Cubic interpolated pseudo-particle method (CIP) for solving hyperbolic-type equations, *Journal of Computational Physics*, Vol.61, pp.261-268, 1985.
10. Takewaki, H., and Yabe, T.: Cubic interpolated pseudo-particle (CIP) method: application to nonlinear and multi-dimensional hyperbolic equations, *Journal of Computational Physics*, Vol.70, pp.355-372, 1987.
11. Eidson, T. M.: Numerical simulation of the turbulent Rayleigh-Benard problem using subgrid modeling, *J. Fluid Mech.*, Vol.158, pp.245-268, 1985.
12. Li, C.W.: Convection of particle thermals, *Journal of Hydraulic Research*, IAHR, Vol.35, No.3, pp.363-376, 1997.
13. Celik, I. and Rodi, W.: Modeling suspended sediment transport in nonequilibrium situations, *Journal of Hydraulic Engineering*, ASCE, Vol.114, No.10, pp1157-1191, 1988.
14. Ying, X., Akiyama, J. and Ura, M.: Motion of dense fluid released into quiescent water with finite depth, *Journal of Hydraulic, Coastal and Environmental Engineering*, JSCE, No.635/II-49, pp.141-152, 1999.

(Received October 2, 2000)